Self-diffusion of a relativistic Lennard-Jones gas via semirelativistic molecular dynamics

David Miles Testa [*], Pontus Svensson, Jacob Jackson, Thomas Campbell, and Gianluca Gregori [†]

Department of Physics, University of Oxford, Parks Road, Oxford OX1 3PU, United Kingdom

The capability for molecular dynamics simulations to treat relativistic dynamics is extended by the inclusion of relativistic kinetic energy. In particular, relativistic corrections to the diffusion coefficient are considered for an argon gas modeled with a Lennard-Jones interaction. Forces are transmitted instantaneously without being retarded, an approximation that is allowed due to the short-range nature of the Lennard-Jones interaction. At a mass density of $1.4\,\mathrm{g/cm^3}$, significant deviations from classical results are observed at temperatures above $k_\mathrm{B}T \approx 0.05\,mc^2$, corresponding to an average thermal velocity of 32% of the speed of light. For temperatures approaching $k_\mathrm{B}T \approx mc^2$, the semirelativistic simulations agree with analytical results for hard spheres, which is seen to be a good approximation as far as diffusion effects are concerned.

I. INTRODUCTION

Starting from Jüttner's seminal work in 1911 on the distribution function of a relativistic gas [1], a number of investigations have appeared on the distribution function [2–4], transport coefficients [4–6], and temperature [3,7–9] of relativistic gases for a variety of interatomic potentials.

At relativistic velocities, any interaction with a considerable range is modified by retardation due to the finite speed of causality. For electromagnetic systems, the interaction can be described only in terms of particle degrees of freedom—to second order in v/c—via the Darwin lagrangian [10–12], an idea which was generalized by Woodcock *et al.* to any scalar interaction [13]. These models only retain interaction terms up to second order in the velocity, something which at least for the Darwin lagrangian does not give the thermodynamics to the same order in the weak interaction limit [14].

One of the key features of a relativistic gas is the relaxation to a Maxwell-Jüttner (MJ) velocity distribution [2,15]

$$f(v)dv \propto v^2 \gamma^5 e^{-\theta\gamma} dv, \tag{1}$$

where v is the magnitude of the three-dimensional velocity, $\gamma(\boldsymbol{v}) = 1/\sqrt{1 - v^2/c^2}$ is the Lorentz factor, $\theta = mc^2/k_\mathrm{B}T$, particle mass m, speed of light c, and $k_\mathrm{B}T$ is the temperature of the gas in energy units. The modification from a classical Maxwell-Boltzmann distribution is solely due to the relativistic expression for kinetic energy. As demonstrated in Ref. [7], any ambiguities in the definition of the gas's temperature are resolved by taking the proper definition of invariant temperature as being the temperature in the comoving frame of the gas. Therefore, the microscopic motion can

be connected to the thermodynamics via comparison with the Maxwell-Jüttner distribution, and the transport properties mapped out by molecular dynamics simulations. Transport properties could in turn inform modeling on a larger length scale, e.g., fluid simulations.

Relativistic dynamics is ubiquitous in both astrophysical and man-made systems. The incorporation of relativistic effects into kinetic theory would assist astrophysics in the study of the thermal history of the universe [16,17] and the cosmic microwave background radiation [18]. Furthermore, relativistic effects are also important in certain approaches to controlled fusion [19].

In the context of nuclear physics, much work has been done on simulating relativistic particle motion and collisions, with software solutions available that also incorporate nuclear effects such as decays and particle production [20–23]. This paper examines the effect of accounting for relativistic kinetic energy on the self-diffusion coefficient of a Lennard-Jones (LJ) gas, and by doing so allows us to introduce an implementation of the relativistic equations of motion in the molecular dynamics software LAMMPS [24]. While our implementation does not contain the nuclear effects captured by Refs. [20–22], it does allow for classical simulations to be conducted in a full range of temperature regimes, from the low temperature classical regime to the high temperature ($k_\mathrm{B}T \approx mc^2$) relativistic. This makes our implementation a useful tool with which to study the transition from classical to relativistic dynamics. While the current study focuses on the LJ interaction, as in Ref. [2], the flexibility of a LAMMPS implementation allows most short-ranged interatomic potential to be inserted easily. The LJ gas in this study has parameters designed to resemble the interaction of atomic argon which for the purpose of this investigation are kept fixed; thermal effects, such as ionization, are not considered.

II. THE MODEL SYSTEM

We investigate a Lennard-Jones gas with the same parameters and density conditions as Rahman [25]—their result is

---

*david.miles.testa@gmail.com

†gianluca.gregori@physics.ox.ac.uk

reproduced in Appendix B—however, for a wider range of temperatures spanning both classical and relativistic systems. Specifically, a periodically repeated cube with side length $L = 30$ Å and $N = 500$ argon atoms (mass per atom $37.2 \, \text{GeV}/c^2$) is simulated, corresponding to a density of $1.374 \, \text{g}/\text{cm}^3$. The system is evolved at constant energy (in the microcanonical ensemble with additional momentum constraints [26]) with an interaction described by the Lennard-Jones pair potential. For two atoms separated by a distance r the interaction energy is

$$V_{\text{LJ}}(r) = 4\varepsilon \left[\left(\frac{\sigma}{r} \right)^{12} - \left(\frac{\sigma}{r} \right)^{6} \right], \qquad (2)$$

and the parameters $\varepsilon = 10.34 \, \text{meV}$ and $\sigma = 3.4$ Å were chosen to mimic the interaction of atomic argon [25,27]. Physically, we can interpret ε as being the depth of the potential, and σ as the size of the atom [28].

As will be noted later, at the relativistic temperatures that we consider, the interactions between atoms may be effectively approximated as a hard-sphere potential with radius r_0. This has two useful consequences. Firstly, the gas with number density $n = N/L^3 \approx 0.02 \, \text{Å}^{-3}$ is characterised as "dilute" at relativistic temperatures since the dimensionless factor

$$\phi = \frac{4\pi}{3} r_0^3 n \approx 10^{-4} \qquad (3)$$

is much less than unity [29], implying collisions at relativistic temperatures are almost exclusively binary, in contrast to the cold regime where significant correlations are observed, see Appendix B.

Secondly, a short-range interaction allows us to ignore post-Newtonian terms in the Hamiltonian, arising from an expansion of a properly Lorentz-invariant theory [13]. For a short-range interaction, the post-Newtonian term is of order $I_{\text{PN}} \sim (v/c)^2 \times V_{\text{LJ}} N/2$, which should be compared to the correction of the kinetic energy introduced $I_{\text{KE}} \sim (v/c)^2 \times mv^2 N/8$. Requiring $I_{\text{PN}} \ll I_{\text{KE}}$ implies

$$V_{\text{LJ}}(r) \ll \frac{mv^2}{4}. \qquad (4)$$

We average the right hand side of Eq. (4) over the Maxwell-Jüttner distribution, then solve for the $r = r^*$ that satisfies Eq. (4) as an equality. This yields the condition $r^* \lesssim \langle r \rangle$, for average interparticle separation $\langle r \rangle \approx 3.6$Å, that we need to be true in order to ignore post-Newtonian terms for most collisions. We numerically calculate r^* using the above process, and the reader is directed to Fig. 3 where r^* is plotted alongside other length scales discussed later in the paper. As is evident from Fig. 3, since $r^* \lesssim 0.6$Å $< \langle r \rangle$ within the temperature range that we study, we neglect all post-Newtonian terms in the Hamiltonian.

By neglecting the post-Newtonian term while retaining the relativistic expression of the kinetic energy, the Hamiltonian of the system follows as $H = T + V$, the sum of kinetic energy T and potential energy V, evaluated in the laboratory frame, which by construction here is also the co-moving frame of the gas [2,8]. Explicitly, the semi-relativistic

Hamiltonian is

$$H = \sum_{i=1}^{N} \sqrt{m^2 c^4 + c^2 |\boldsymbol{p}_i|^2} + \sum_{j>i}^{N} V_{LJ}(|\boldsymbol{r}_j - \boldsymbol{r}_i|), \qquad (5)$$

in terms of position $\boldsymbol{r}_i$ and canonical momentum $\boldsymbol{p}_i = \gamma_i m \boldsymbol{v}_i$ of the ith particle. The equations of motion follow readily [2] as

$$\frac{d\boldsymbol{r}_i}{dt} = \frac{\boldsymbol{p}_i}{m\gamma_i} \qquad (6a)$$

and

$$\frac{d\boldsymbol{p}_i}{dt} = -\sum_{\substack{j=1 \\ j \neq i}}^{N} \frac{dV_{LJ}(|\boldsymbol{r}_j - \boldsymbol{r}_i|)}{d\boldsymbol{r}_i}, \qquad (6b)$$

where $\gamma_i = \gamma(\boldsymbol{v}_i)$ is the Lorentz factor for the ith particle. Within the simulation, Eq. (6) is discretized according to a second-order symplectic velocity-Verlet scheme and expressed fully in terms of velocity, the details of which are described in Appendix A.

The nonrelativistic reference system—hereafter referred to as the classical system—is described by the standard Hamiltonian

$$H_{\text{cl}} = \sum_{i=1}^{N} \frac{\boldsymbol{p}_i^2}{2m} + \sum_{j>i}^{N} V_{\text{LJ}}(|\boldsymbol{r}_j - \boldsymbol{r}_i|), \qquad (7)$$

yielding the classical equations of motion

$$\frac{d\boldsymbol{r}_i}{dt} = \frac{\boldsymbol{p}_i}{m}, \qquad (8)$$

where the momentum equation takes the same form as in Eq. 6(b).

Finally, implicit in the above Hamiltonian is the assumption that particle creation/annihilation processes are ignored, as no explicit treatment of the background radiation field is included and a constant number of particles is assumed.

III. SELF-DIFFUSION COEFFICIENT

In the continuous, nonrelativistic fluid limit, the self-diffusion coefficient D governs how gradients in the local density $\rho(\boldsymbol{x})$ of a quantity lead to flow, via Fick's law [28]

$$\frac{d\rho}{dt} = -\boldsymbol{\nabla} \cdot (D \boldsymbol{\nabla} \rho). \qquad (9)$$

The diffusion coefficient itself $D = D(n, T, \sigma, \varepsilon, \dots)$ is a material property depending on the underlying interaction between particles and the structure of the system considered. As shown in Ref. [30], Eq. (9) is incompatible with special relativity, as it allows for superluminal transport. A number of candidate models for relativistic diffusion exist [31–33] although the topic is still debated [34]. An in-depth discussion of the topic is beyond the scope of the current manuscript, but the interested reader is directed to Ref. [34] for a review of the subject. As noted in Ref. [35], the breakdown of the diffusion equation occurs at small wavelengths beyond the region of validity of a hydrodynamic description. Therefore, limiting ourselves to Eq. (9) and hydrodynamic scales, the issue of

causality can largely be avoided. A benefit of using the form of Eq. (9) is that this form allows the diffusion coefficient to be calculated via the Green-Kubo formula [28,36]

$$D = \lim_{t \to \infty} \frac{\langle |\boldsymbol{r}_i(t) - \boldsymbol{r}_i(0)|^2 \rangle}{6t}$$
$$= \frac{1}{3} \int_0^\infty \langle \boldsymbol{v}_i(t) \cdot \boldsymbol{v}_i(0) \rangle dt \qquad (10)$$

for any particle i in an N body ensemble, as the diffusion coefficient is directly related to the mean square displacement of particles in the rest frame of the overall gas. Here the angle bracket $\langle \cdot \rangle$ denotes an ensemble average or thermal average, which by the ergodic hypothesis can be identified as a time average in molecular dynamics [15]. The integrand in Eq. (10) is known as the velocity autocorrelation function (VACF), and represents how quickly the information about the atom's initial velocity is lost [28].

To compute the diffusion coefficient, the atoms were initialized at random positions and the potential energy was minimized by a line search to find a stable starting configuration. The velocities were set all to equal magnitude in random directions without net momentum and the system is evolved in time according to Sec. II. Momentum conservation guarantees the system stays in the comoving frame of the gas, thus allowing us to measure the invariant temperature by fitting the distributions of particle speeds to Eq. (1).

The time average of the velocity autocorrelation function was sampled based on 100 different time origins over the course of each simulation allowing for a 50 000 time-step gap between measurements to reduce correlations between samples. The time step was adjusted for each simulation as well as the length of time over which data was collected. This is to guarantee appropriate energy conservation and the convergence of Eq. (10). A typical time step in the relativistic regime was on the order of zeptoseconds (10^{-21} s), and a typical VACF measurement would run for 3 000 000 time-steps (3 fs) where for every 100 time-steps the dot product in Eq. (10) was carried out for all the particles in the system. This was done every 100 time-steps, as the time step required for time integration is far below the needed resolution of the VACF.

A decaying exponential was fitted to the VACF data to limit the impact of noise on the computation of the diffusion coefficient [37]. An example VACF calculation is shown in Fig. 1. Given an exponential fit, the diffusion coefficient can be explicitly evaluated in terms of fitting parameters, the result of which is shown in Fig. 2.

The diffusion coefficient of a relativistic hard-sphere gas can be calculated based on the work by Kremer [5]. Modified for flat Minkowski space, without gravitational potential, and only a single species self-diffusing, Kremer's analytical model results in a diffusion coefficient

$$D_{\text{Kremer}} = \frac{3c}{16\pi n \sigma_T} \frac{\theta K_2(\theta)^2}{7K_3(2\theta) + K_2(2\theta)(2\theta + \theta^{-1})} \qquad (11)$$

based on the constant differential scattering cross-section σ_T at a given temperature. The two functions K_2 and K_3 are the second- and third-order Bessel functions of the second kind
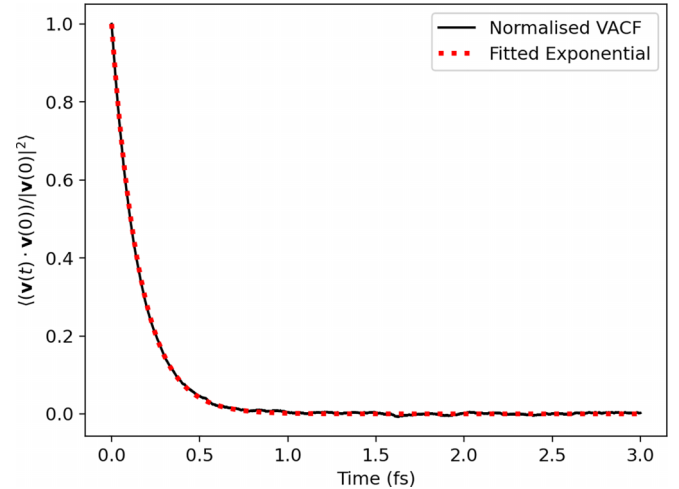

FIG. 1. The velocity autocorrelation function at $k_B T = 0.014 \, mc^2$, normalized to $|\boldsymbol{v}(0)|^2 = 3.5 \times 10^{15} \, \mathrm{m^2 s^{-2}}$. The average molecular dynamics data (solid) is shown alongside an exponential fit (dashed) which describes the data throughout the full range.

respectively. Assuming hard-sphere interactions [5]

$$\sigma_T = r_0^2 \qquad (12)$$

for the effective interaction range $2r_0$ twice the radius of an atom in the hard-sphere model.

At relativistic temperatures, the LJ potential with its short range and steep repulsive core effectively acts as a hard-sphere potential. To find an appropriate scale of r_0, the average kinetic energy $\langle mc^2(\gamma - 1) \rangle$ [38] is equated to the LJ interaction
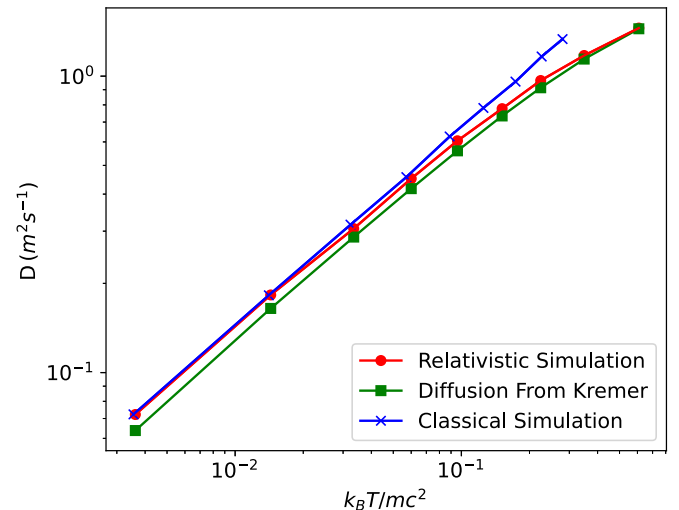

FIG. 2. Diffusion coefficients from the classical molecular dynamics (crosses), relativistic molecular dynamics (dots), and calculated via Eq. (11) (squares) using Eq. (12) as the cross-section. Here the diffusion coefficient D is plotted as a function of the temperature in units of the atom's rest mass energy. The relativistic computation goes from agreement with the classical simulations at low temperatures to agreement with relativistic hard spheres in the opposite limit. Error bars on the data—estimated by the uncertainty in the fit—are smaller than the marker.
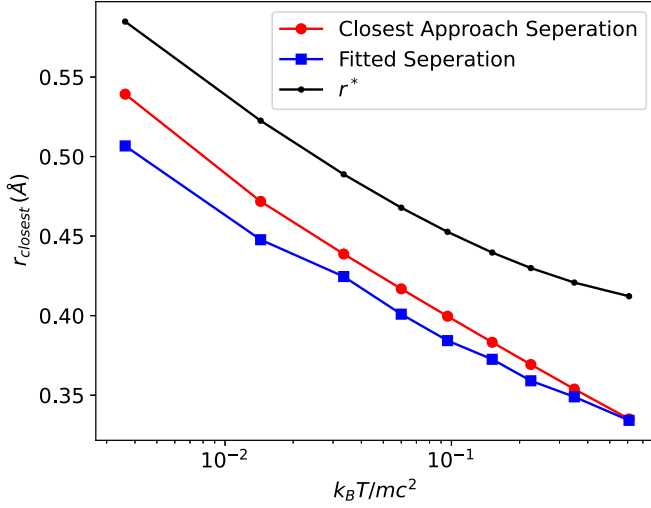
FIG. 3. The separation r_{closest} (dots) defined in Eq. (13) compared to the $2r_0$ needed for the diffusion coefficient by Kremer, Eq. (11), to reproduce the result of the relativistic simulation (squares). The two separations converge at high enough temperatures, indicating the gas is well approximated as a hard-sphere system. The length scale r^* (small dots) needed to satisfy Eq. (4) is also plotted for reference.

energy, a condition which is satisfied at a separation

$$r_{\text{closest}} = 2^{\frac{1}{6}}\sigma \left(1 + \sqrt{1 + \frac{mc^2}{\varepsilon}(\langle \gamma \rangle - 1)} \right)^{-1/6} \equiv 2r_0. \quad (13)$$

The average gamma factor is computed by numerical integration over the MJ distribution.

The resulting diffusion coefficients are shown in Fig. 2 where the classical and relativistic simulations are seen to agree for low temperatures. The analytical model gives the correct trends in this limit, but the hard-sphere approximation is not good enough to give a quantitative agreement. In the high-temperature limit, on the other hand, agreement is shown between the relativistic data and the analytical model where the hard-sphere approximation is appropriate. The relativistic correction to the kinetic energy becomes appropriate for this system at $k_{\text{B}}T \approx 0.05\,mc^2$ where the two numerical calculations start to diverge.

Figure 3 shows the analytical model for closest separation r_{closest} and the r_0 value obtained by requiring that Kremer's analytical model matches the simulation data. The two distances converge for high temperatures, confirming that at least for the computation of diffusion coefficients where retarded interactions are ignored, the LJ gas can be well approximated as a system of hard spheres.

IV. CONCLUSIONS

The implementation of a relativistic Lennard-Jones gas simulation with instantaneous force transmission is realised in LAMMPS, by the addition of relativistic kinetic energy to the equations of motion. The tool is used for the computation of diffusion coefficients of a Lennard-Jones gas over a wide range of temperatures, which is compared with computations for a classical gas and analytical model for hard spheres by Kremer [5]. In particular, the Lennard-Jones interaction

was chosen to resemble the interaction between two atoms of argon. The semirelativistic and classical results diverged from one another as temperatures approached the weakly relativistic regime, parting noticeably around a temperature of $k_{\text{B}}T \approx 0.05\,mc^2$. Our semirelativistic results approach those predicted by Kremer as the temperature rise, suggesting that the hard sphere approximation is appropriate and the instantaneous force transmission approximation has a limited impact.

Having established the methods described in this paper, further work could be done on calculating the transport coefficients of a relativistic LJ gas, such as the coefficient of viscosity. Conceivably, these methods could also be applied to any relativistic gas with a potential that has an effective range r_0 such that post-Newtonian corrections can be neglected. One possible candidate would be the Yukawa potential [39] for suitable parameter choices, though further analysis would be required.

A treatment of long-range interactions that accounts for retarded effects is still outstanding. Such a treatment would be highly desirable for high-temperature applications where relativistic effects are important, and the gas has ionized to a plasma.

APPENDIX A: DISCRETIZED EQUATIONS OF MOTION

The equations of motion for the gas particles have been discretized via a velocity-Verlet integration scheme [28], the most commonly used for molecular dynamics simulations due to its performance with respect to energy conservation [40]. In the following derivation, superscripts are used to designate the time-step (e.g., $\boldsymbol{p}_i^k$ is the momentum of the ith particle at the kth time-step). Note a superscript $k + \frac{1}{2}$ corresponds to a half step in time.

Equation (6) is advanced half a time step by

$$\boldsymbol{p}_i^{k+1/2} = \boldsymbol{p}_i^k - \frac{dt}{2}\frac{dV}{d\boldsymbol{r}_i^k} \equiv \boldsymbol{p}_i^k + \frac{dt}{2}\boldsymbol{F}_i^k \quad (A1)$$

and the definition of γ in terms of momentum [38] can then be used to update the velocity

$$\boldsymbol{v}(\boldsymbol{p}) = \frac{\boldsymbol{p}/m}{\sqrt{1 + |\boldsymbol{p}|^2/(mc)^2}} \quad (A2)$$

and the position

$$\boldsymbol{r}_i^{k+1} = \boldsymbol{r}_i^k + \frac{dt}{m}\boldsymbol{v}\left(\boldsymbol{p}_i^{k+1/2}\right) \quad (A3)$$

by a whole time-step. These positions are used to update the force $\boldsymbol{F}_i^{k+1}$. The final step in the discretization scheme is to update the momentum by another half step

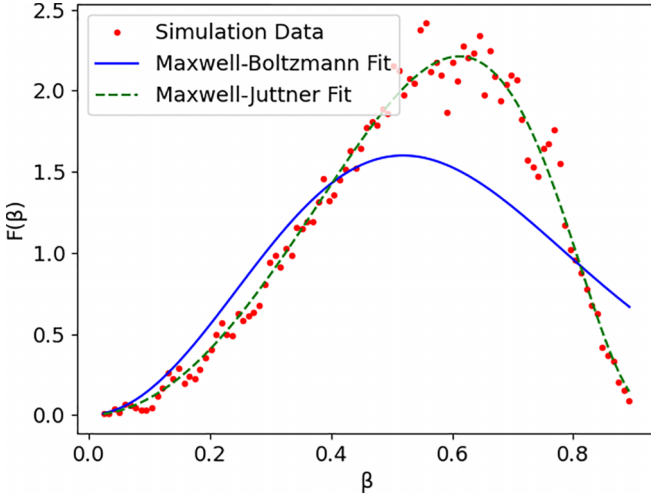$$\boldsymbol{p}_i^{k+1} = \boldsymbol{p}_i^{k+1/2} + \frac{dt}{2}\boldsymbol{F}_i^{k+1}, \quad (A4)$$

FIG. 4. Velocity distribution of a LJ gas with $k_B T = 0.014mc^2$ in terms of normalized velocity $\beta = v/c$. Lines are fitted with Maxwell-Jüttner (dashed) and Maxwell-Boltzmann (solid) distributions respectively.

resulting in a scheme which can be shown to be second order in dt and symplectic [40].

When inserting these equations of motion into LAMMPS, they are recast in terms of velocity rather than momentum. Using the definitions for p and γ in terms of velocity, these two variables are discretized as

$$p_i^{k+1} = m\gamma^{k+1}v_i^{k+1} \, and \tag{A5a}$$

$$\gamma_i^k = \frac{1}{\sqrt{1 - v_i^k \cdot v_i^k/c^2}}. \tag{A5b}$$

Inserting these definitions into the above velocity-Verlet scheme, we arrive at

$$v_i^{k+1/2} = \Gamma^{-1}\left(v_i^k, \gamma_i^k, F_i^k\right)\left(\gamma_i^k v_i^k + \frac{dt}{2m}F_i^k\right),$$

$$r_i^{k+1} = r_i^k + dt\, v_i^{k+1/2},$$

$$v_i^{k+1} = \Gamma^{-1}\left(v_i^{k+1/2}, \gamma_i^{k+1/2}, F_i^{k+1}\right)$$

$$\times \left(\gamma_i^{k+1/2}v^{k+1/2} + \frac{dt}{2m}F_i^{k+1}\right) \tag{A6}$$

where

$$\Gamma(v, \gamma, F) = \sqrt{1 + c^{-2}\left[\gamma v + \frac{dt}{2m}F\right]^2}. \tag{A7}$$

The implementation was validated by the reproduction of the Maxwell-Jüttner distribution—see Fig. 4—when operating at relativistic temperatures and the absence of any significant energy drift during the simulation.

APPENDIX B: REPRODUCING RAHMAN (1964)

The system was equilibrated close to the temperature of Rahman's original work [25], in this case 92.86 K, and the radial distribution function $g(r)$ defined by [28]

$$g(r) = \frac{\langle N_{[r,r+dr]}\rangle}{nV_{[r,r+dr]}} \tag{B1}$$

was computed. Here $N_{[r,r+dr]}$ is the number of atoms within a shell of width dr at a distance r from a specific atom, the volume of which is $V_{[r,r+dr]}$. The radial distribution function is a measure of the average local density around each atom in the system. During the simulation, the radial distribution function was measured each picosecond, and averaged every 10 picoseconds. Figure 5 shows the radial distribution function by Rahman alongside the present work, with good agreement. The VACF was also computed for this system but did not exhibit any obvious exponential decay and was numerically integrated for the computation of the diffusion coefficient. By the error analysis in Ref. [37], the error, in this case, is estimated to the order of 5%, yielding a value of the diffusion coefficient $D = 2.44 \pm 0.12 \times 10^{-9}m^2s^{-1}$ almost identical to that found in the original paper, $2.43 \times 10^{-9}m^2s^{-1}$.
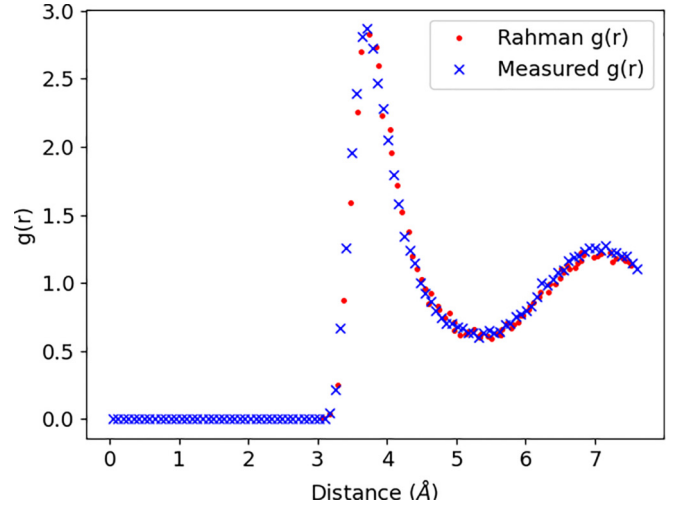

FIG. 5. Radial distribution function for the LJ gas at 92.86 K with significant correlations. Good agreement with Ref. [25] (dots) and the present work (crosses) are shown.

[1] F. Jüttner, Das maxwellsche gesetz der geschwindigkeitsverteilung in der relativtheorie, Ann. Phys. **339**, 856 (1911).

[2] A. Aliano, L. Rondoni, and G. P. Morriss, Maxwell-jüttner distributions in relativistic molecular dynamics, Eur. Phys. J. B **50**, 361 (2006).

[3] M. Ghodrat and A. Montakhab, Molecular dynamics simulation of a relativistic gas: Thermostatistical properties, Comput. Phys. Commun. **182**, 1909 (2011).

[4] G. M. Kremer, On the kinetic theory of relativistic gases, Continuum Mech. Thermodyn. **9**, 13 (1997).

[5] G. M. Kremer, Diffusion of relativistic gas mixtures in gravitational fields, Physica A **393**, 76 (2014).

[6] G. M. Kremer, Relativistic gas in a schwarzschild metric, J. Stat. Mech. (2013) P04016.

[7] G. Chacón-Acosta, L. Dagdug, and H. A. Morales-Técotl, Manifestly covariant jüttner distribution and equipartition theorem, Phys. Rev. E **81**, 021126 (2010).

[8] N. Kubli and H. J. Herrmann, Thermostat for a relativistic gas, Physica A **561**, 125261 (2021).

[9] S. Groot, W. Leeuwen, C. van Weert, and C. Weert, *Relativistic Kinetic Theory: Principles and Applications* (North-Holland Publishing Company, 1980).

[10] C. G. Darwin, Li. the dynamical motions of charged particles, Lond. Edinb. Dublin Philos. Mag. J Sci. **39**, 537 (1920).

[11] J. D. Jackson, *Classical Electrodynamics* (Wiley, 1999).

[12] L. Landau and E. Lifshitz, The classical theory of fields, course of theoretical physics (1971).

[13] W. N. Herman and P. Havas, Approximately Relativistic Lagrangians for Classical Interacting Point Particles. III, Phys. Rev. D **17**, 1985 (1978).

[14] X. Barcons and R. Lapiedra, Statistical mechanics of classical dilute relativistic plasmas in equilibrium, J. Phys. A: Math. Gen. **18**, 271 (1985).

[15] R. L. Liboff, *Kinetic theory: classical, quantum, and relativistic descriptions* (Springer Science & Business Media, 2003).

[16] J. Bernstein, *Kinetic theory in the Expanding Universe*, Cambridge Monographs on Mathematical Physics (Cambridge University Press, Cambridge, UK, 1988).

[17] J. Peacock and C. U. Press, *Cosmological Physics*, Cambridge Astrophysics (Cambridge University Press, 1999).

[18] R. A. Sunyaev and Y. B. Zeldovich, The Observations of relic radiation as a test of the nature of x-ray radiation from the clusters of galaxies, Comments Astrophys. Space Phys. **4**, 173 (1972).

[19] A. H. Boozer, Theory of runaway electrons in ITER: Equations, important parameters, and implications for mitigation, Phys. Plasmas **22**, 032504 (2015).

[20] J. Weil, V. Steinberg, J. Staudenmaier, L. G. Pang, D. Oliinychenko, J. Mohs, M. Kretz, T. Kehrenberg, A. Goldschmidt, B. Bäuchle, J. Auvinen, M. Attems, and H. Petersen, Particle production and equilibrium properties within a new hadron transport approach for heavy-ion collisions, Phys. Rev. C **94**, 054905 (2016).

[21] S. Bass, Microscopic models for ultrarelativistic heavy ion collisions, Prog. Part. Nucl. Phys. **41**, 255 (1998).

[22] M. Bleicher, E. Zabrodin, C. Spieles, S. A. Bass, C. Ernst, S. Soff, L. Bravina, M. Belkacem, H. Weber, H. Stöcker, and W. Greiner, Relativistic hadron-hadron collisions in the ultra-relativistic quantum molecular dynamics model, J. Phys. G: Nucl. Part. Phys. **25**, 1859 (1999).

[23] H. Sorge, H. Stöcker, and W. Greiner, Poincaré invariant hamiltonian dynamics: Modelling multi-hadronic interactions in a phase space approach, Ann. Phys. **192**, 266 (1989).

[24] S. Plimpton, A. Kohlmeyer, A. Thompson, S. Moore, and R. Berger, Lammps stable release 29 october 2020 (2020).

[25] A. Rahman, Correlations in the motion of atoms in liquid argon, Phys. Rev. **136**, A405 (1964).

[26] K. Meier and S. Kabelac, Pressure derivatives in the classical molecular-dynamics ensemble, J. Chem. Phys. **124**, 064104 (2006).

[27] J.-P. Hansen and I. R. McDonald, *Theory of simple liquids: with applications to soft matter* (Academic press, 2013), Chap. 1.

[28] D. C. Rapaport and D. C. R. Rapaport, *The art of molecular dynamics simulation* (Cambridge university press, 2004).

[29] R. Soto, *Kinetic Theory and Transport Phenomena* (Oxford University Press, 2016).

[30] P. Kostädt and M. Liu, Causality and stability of the relativistic diffusion equation, Phys. Rev. D **62**, 023003 (2000).

[31] T. Koide, Microscopic derivation of causal diffusion equation using the projection operator method, Phys. Rev. E **72**, 026135 (2005).

[32] T. Koide, Microscopic formula for transport coefficients of causal hydrodynamics, Phys. Rev. E **75**, 060103(R) (2007).

[33] J. Masoliver and G. H. Weiss, Finite-velocity diffusion, Eur. J. Phys. **17**, 190 (1996).

[34] J. Dunkel and P. Hänggi, Relativistic brownian motion, Phys. Rep. **471**, 1 (2009).

[35] W. Florkowski, M. P. Heller, and M. Spaliński, New theories of relativistic hydrodynamics in the LHC era, Rep. Prog. Phys. **81**, 046001 (2018).

[36] R. Kubo, The fluctuation-dissipation theorem, Rep. Prog. Phys. **29**, 255 (1966).

[37] J. Mithen, J. Daligault, and G. Gregori, Molecular dynamics simulations for the shear viscosity of the one-component plasma, Contrib. Plasma Phys. **52**, 58 (2012).

[38] A. M. Steane, *Relativity made relatively easy* (Oxford University Press, 2012).

[39] H. YUKAWA, On the interaction of elementary particles. I, Proc. Phys. Math. Soc. Jpn. **17**, 48 (1935).

[40] B. Leimkuhler and S. Reich, *Simulating Hamiltonian Dynamics*, Cambridge Monographs on Applied and Computational Mathematics (Cambridge University Press, 2004).